Received 2 July 2019; revised 14 September 2019; accepted 15 September 2019. Date of publication 18 September 2019; date of current version 30 September 2019. The review of this article was arranged by Editor C. Bulucea.

Digital Object Identifier 10.1109/JEDS.2019.2942188

Modeling of the Variation of Lateral Doping (VLD) Lateral Power Devices via 1-D Analysis Using Effective Concentration Profile Concept

JUN ZHANG [1,2] (Member, IEEE), YU-FENG GUO [1,2] (Member, IEEE), KE-MENG YANG [1,2] (Student Member, IEEE), CHEN-YANG HUANG [1,2], AND FANG-REN HU [1,2]

1 College of Electronic Science and Engineering, Nanjing University of Posts and Telecommunications, Nanjing 210003, China
2 National and Local Joint Engineering Laboratory for RF Integration and Micro-Packaging Technologies, Nanjing University of Posts and Telecommunications, Nanjing 210003, China

CORRESPONDING AUTHOR: Y.-F. GUO (e-mail: yfguo@njupt.edu.cn)

This work was supported in part by the China Post-Doctoral Science Foundation under Grant 2018M642291, in part by the Natural Science Foundation of Jiangsu Province under Grant SBK2019041165, and in part by the National Natural Science Foundation of China under Grant 6190030245, Grant 61574081, and Grant 61704084.

ABSTRACT The VLD technique has introduced for the propose of achieving the ideal surface electric field via a non-uniformly doped drift region. Yet, the ideal doping profile is impossible to be fulfilled in practical thus breaking the optimized lateral breakdown characteristic. In addition, the conventional 2-D methods, due to its complexity, are impractical in both explaining its physical nature and providing designing guidance. In this paper, a simple 1-D methodology based on Effective Concentration Profile (ECP) theory is proposed to provide the physical insight of the VLD technique and quantitatively depict its breakdown characteristic. The VLD-ECP concept indicates that the perfectly even surface electric field can be obtained by adjusting the drift region doping dose equals to the Charge Appointment Line (CAL) so that all the charges in drift region contribute to the vertical depletion, thus the lateral structure being an equivalently P-I-N junction. Considering non-ideal doping profile of commercial devices, a designing optimization criterion is proposed to avoid the undesirable lateral breakdown. The analytical results obtained by the proposed model are found to be sufficiently accurate comparing with TCAD simulation results verifying the veracity and effectiveness of the proposed methodology.

INDEX TERMS Variation of lateral doping, effective concentration profile, 1-D breakdown theory, breakdown voltage.

I. INTRODUCTION

The Reduce Surface Electric Field (RESURF) technique reduces the surface electric field peaks and improves the device's breakdown characteristic by coupling two or more depletion region [1]–[5]. For the Single-RESURF lateral power devices, such coupling between lateral and vertical structure reduces the charge that contributes to the lateral depletion and therefore equivalently reduces the surface electric field. To utilize the 2-D coupling effect, many techniques such as Double/Triple/Multi-RESURF, Variation of Lateral Doping (VLD), Variable of Lateral Width (VLW) and Variable of Lateral Thickness (VLT) have been introduced to alter the charge distribution or doping dose ($Q(x) = N_d(x) \times t_s(x)$) of the drift region [6]–[9]. So that a better trade-off between breakdown voltage (BV) and specific on-resistance (Ron) can be achieved. Among them, the VLD structure features for its linearly doped drift region therefore capable of achieving the perfectly even surface electric field and obtaining the maximum lateral BV in theory. However, due to the inherent doping concentration of the epitaxial layer, the realization of the ideal proportionally doping profile ($N_d(x) = ax$) is hard to accomplish in a commercial scenario [6], [7], [9]. In fact, the actual doping concentration at the PN junction ($x = 0$) is impossible to be down to zero. Even though, due to the lightly doped region near the PN junction, the VLD devices are inevitably to have severe local self-heating and deteriorated on-state characteristic. Therefore, in order to maintaining a high BV and low Ron simultaneously, the actual lateral doping profile ought to be optimized [10]–[12]. However, due to the complexity of the conventional 2-D approaches, the modeling and analysis on the influence of non-uniform doping profile on the surface electric field and BV characteristic via directly solving 2-D Poisson's equation are already impractical [11]–[14]. Not to mention to provide physical insights on how the lateral doping affects the lateral BV characteristic.

In this paper, for the non-uniformly doped drift region, the ECP concept is employed to explain the physical nature and provide designing guidance for the VLD devices. The VLD-ECP concept indicates that the 2-D coupling effect between the lateral and vertical structure is independent of the lateral doping profile. Thus, the influences of lateral doping and 2-D coupling can be simultaneously considered using the principle of compensational doping. Based on the VLD-ECP concept, a 1-D analytical model is proposed to depict the surface electric field profile and breakdown characteristic of the lateral power devices with the arbitrary lateral doped drift region. The effectiveness of the proposed methodology is validated by the good agreement between the analytical results and simulations by MEDICI, technology computer-aided design (TCAD) tool. Moreover, a simple optimization method is proposed to provide design guidance for the practical VLD lateral power devices considering the non-ideal conditions. The simulation models used in MEDICI are CONSRH, AUGER, BGN, FLDMOB, IMPACT.I and CCSMOB.

II. ARBITRARY LATERAL DOPING MODEL

One of the distinguishing features of the lateral power devices is its capability of handling high voltage when operates in off-state. Such a feature is realized by the depletion of the lowly doped region and thus the drift region doping plays a decisive role in affecting the device's BV characteristic. To qualitatively and quantitatively explore the sensitivity of the surface electric field and breakdown voltage to structure parameters especially the drift region doping dose, as shown in Fig. 1 (a), the 2-D cross-section of the lateral power device with arbitrary doping concentration $N(x)$ is applied for modeling. The breakdown may occur on lateral PN junction, lateral NN junction or vertical structure as indicated by point A, B, and C, respectively. Instead of solving complicated 2-D Poisson's equation directly, the proposed ECP concept depicts the complicated 2-D device by reducing which into a 1-D structure. The core idea of the ECP concept is to equivalent the inherent 2-D device to a simple abrupt 1-D planar junction with variable doping profile [4], [6]. In which case, the 2-D effects and their coupling relationship can be easily represented by the fluctuation of the ECP. According to the principle of compensation semiconductor, for the lateral power devices with arbitrary lateral doped drift region, both non-uniform doping and 2-D coupling effect influence the ECP. Accordingly, the 2-D VLD device can be simply equivalent to an abrupt 1-D planar junction with varied drift region doping profile, and thus the effective concentration profile ($N_{eff}(x)$) of the drift region can be expressed as:

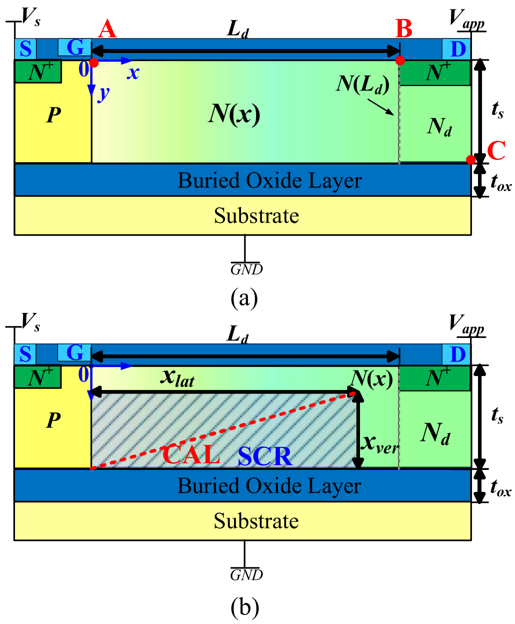

FIGURE 1. (a). 2-D cross-section and (b). ECP equivalent structure of the SOI LDMOS with VLD structure (*x*-*y* plane).

$$N_{eff}(x) = N(x) + \Delta N_{eff-RESURF} \tag{1}$$

where $\Delta N_{eff-RESURF} = -\eta x N_d / Min[x_{lat}, L_d]$ indicates the influence of the 2-D coupling effect on ECP [4]. In this paper, $\eta = x_{ver}(V_{app})/t_s$ is the ratio of vertical depletion length at $x = Min[x_{lat}, L_d]$ and SOI layer thickness. The N_d being the doping concentration under the drain region. In practice, considering the fabrication process, the N_d usually equals to $N(L_d)$. Thus, in this paper, unless otherwise stated, $N_d = N(L_d)$. As shown in Fig. 1 (b), due to the depletion region expands both along the lateral and vertical direction. An overlapped depletion region, namely Sharing Charge Region (SCR) is therefore formed. The boundary of the SCR is limited by the width of the lateral and vertical depletion region, namely x_{lat} and x_{ver}, respectively. According to ECP theory, as shown in Fig. 1 (b) a Charge Appointment Line (CAL(x) $= \eta x N_d / Min[x_{lat}, L_d]$) can be applied to illustrate the inherent 2-D coupling effect by separating the SCR into two parts, and only the upper part contributes to the lateral depletion [4], [6]. Namely, with the help of charge sharing in the SCR, the equivalent doping concentration for the lateral depletion is reduced. Thus, the depletion expansion along the surface is promoted accordingly so that a better surface electric field and lateral BV can be achieved.

To obtain the ideal lateral BV characteristic, the surface electric field ought to be even when the lateral breakdown occurs. In which case, the lateral BV is only determined by

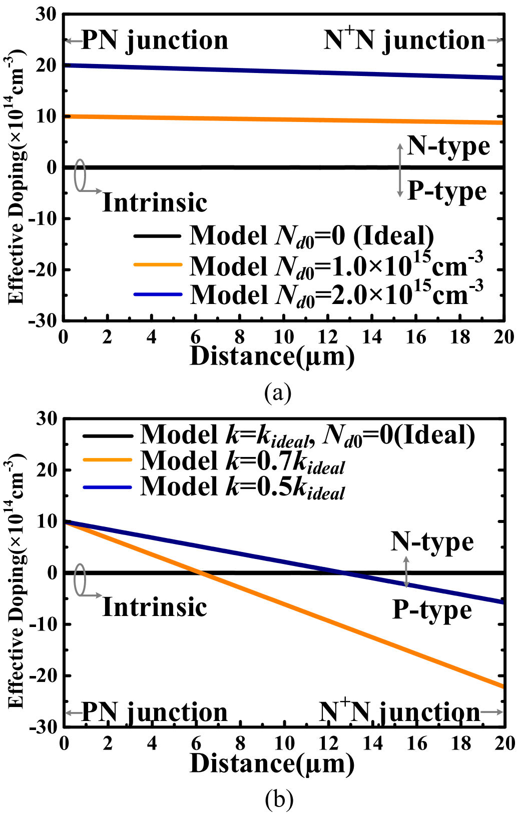

FIGURE 2. Effective Doping Concentration of the drift region for various (a). Epitaxial layer doping concentration ($V_{app} = 400$ V, $k = 4.1 \times 10^{18}\text{cm}^{-4}$) and (b). Doping gradient of the drift region ($V_{app} = 400$V, $N_{d0} = 1.0 \times 10^{15}\text{cm}^{-3}$) with $t_s = 3\mu$m, $t_{ox} = 3\mu$m, $L_d = 20\mu$m.

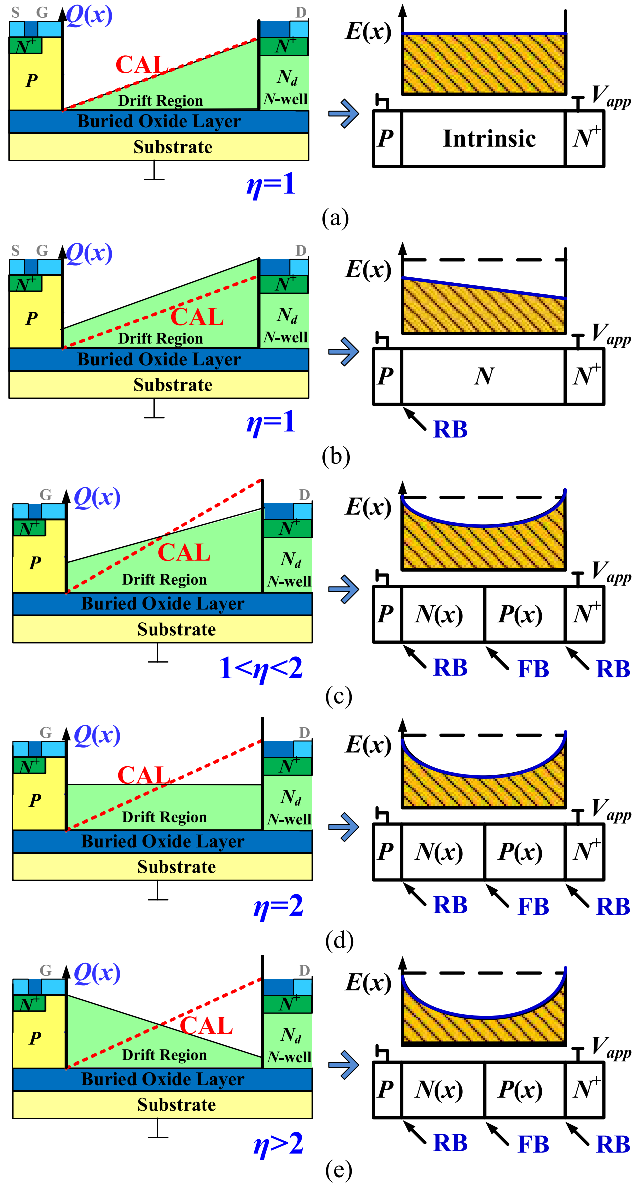

FIGURE 3. Equivalent charge distribution and the electric field distribution of the VLD device with: (a). Intrinsic, (b). N-type, (c). NP-type drift region (N_{d0} <CAL(L_d/2), η <2) , (d). NP-type drift region (N_{d0} = CAL(L_d/2), $\eta = 2$) and (e). NP-type drift region (N_{d0} > CAL(L_d/2), $\eta > 2$) (RB: Reverse-Biased, FB: Forward-Biased).

the critical electric field (E_C) and drift region length (L_d). Namely, the drift region is fully depleted and the breakdown voltage of the lateral structure achieves $BV_{lat\_Max} = E_C \times L_d$. To do so, the ECP ought to satisfy $N_{eff}(x) = 0$. For VLD lateral power devices, the doping gradient of the drift region ($k = \Delta N(x)/\Delta x$) plays a decisive role in affecting the drift region's ECP. By using Eq. (1), the ideal doping profile of the drift region can be easily obtained, which yields:

$$N_{ideal}(x) = \left(\eta \frac{N_d}{L_d}\right)x \tag{2}$$

Accordingly, the ideal k_{ideal} ought to satisfies $k_{ideal} = \eta N_d/L_d$. By using the expression of the vertical voltage in REF [4], [5], the ideal doping profile defined by Eq. (2) can be re-written to a more commonly seen form, $N_{ideal}(x) = \varepsilon_s E_C/qt^2x$ thus verifying the correctness of the proposed methodology. It is worth to be noted that in which case the 2-D coupling factor $\eta = 1$ indicating that the drift region is just fully depleted when the ideal lateral BV being achieved ($x_{lat} = L_d$). However, despite the even surface electric field and ideal lateral BV that ideal doping profile brings, as mentioned above, its realization is impractical in practice. Due to the impurities introduced during the epitaxial growth process, the drift region already has the epitaxial layer doping concentration (N_{d0}) before forming the VLD region. In which case, the actual doping concentration is $N(x) = kx + N_{d0}$. As shown in Fig. 2, these extra charges significantly harm the fragile balance between the doping profile and charge sharing line. Nevertheless, as indicated in Eq. (1), the ECP increment induced by 2-D coupling effect between lateral and vertical structures only determined by the doping concentration of the epitaxial layer below the drain region and irrelevant to the doping profile of the drift region. Thus, as shown in Fig. 2 and Fig. 3, by adjusting the doping gradient of the drift region, although the perfectly even surface electric field still cannot be achieved, another electric field peak at N^+N junction is expected to be formed. Fig. 3 intuitively shows the 2-D charge sharing in drift region and corresponding 1-D ECP structure. As shown in Fig. 3 (a), the ideal equivalent PIN structure is achieved only when the doping of drift region is just fitting the CAL(x) meaning the charge in the drift region has no contribution to the lateral depletion. In which case, the drift region doping is equivalently intrinsic, so that the perfectly even surface electric field occurs. Yet, as shown in Fig. 3 (b), due to the extra charges from epitaxial layer impurity, the actual doping dose of drift region excesses the CAL(x) and therefore forms an equivalent PNN structure leading to an electric field peak formed at PN junction. By utilizing the mismatch between doping profile and 2-D coupling when $\eta > 1$, as shown in Fig. 3 (c), the cross between CAL(x) and $Q(x)$ creating an equivalent N(x)P(x) drift region which leads to electric filed peaks both at PN and N^+N junctions. Compared to the case shown in Fig. 3 (b), the equivalent N(x)P(x) structure allows an evener surface electric field profile and improves the lateral BV characteristic. As shown in Fig. 3 (d), when $N_{d0} = \mathrm{CAL}(L_d/2)$, the 2-D coupling factor equals to 2. In which case, the optimized lateral doping profile ought to satisfies $N(x) = N_d$. and the VLD structure is degenerate into a Single-RESURF structure. Moreover, when $N_{d0} = \mathrm{CAL}(L_d/2)$, namely $\eta > 2$, the optimized lateral doping profile returns to a linear function. However, as shown in Fig. 3 (e), the gradient of lateral doping in which case has a negative value. This case occurs when the inherent epitaxial layer doping concentration is too high so that the P-type doping ought to be introduced to neutralize the extra charges near the NN^+ junction. Obviously,

So far, by applying the ECP concept, the influence of 2-D coupling and non-uniformed drift region doping are both reflected by the fluctuation of ECP. Therefore, the inherent 2-D structure of the lateral power device with arbitrary lateral doping can be equivalent to a simple 1-D diode with ECP. So that, the sophisticated modeling process of 2-D methods can be bypassed and the surface electric potential [$\varphi(x,0)$] and electric field [$E(x,0)$] can be described by directly solving 1-D Poisson's equation yielding [4], [5]:

$$\frac{d^2\varphi(x,0)}{dx^2} = \frac{dE(x,0)}{dx} = -\frac{qN_{eff}(x)}{\varepsilon_s} \tag{3}$$

Accordingly, the surface electric field profile of the devices with arbitrary lateral doping can be easily obtained by submitting Eq. (1) into Eq. (3), which yields:

$$E(x) = E_0 - \frac{qN_d}{\varepsilon_s}\left[\int \frac{N(x)}{N_d}dx - \eta\frac{x^2}{2L_d}\right] \tag{4}$$

where $E_0 = E(0)$ represent the surface electric field at PN junction. When $N(x)$ in accordance with Eq. (2), the Eq. (4) satisfies $E(x) = E_0$ meaning the ideal lateral BV is obtained. The lateral breakdown voltage can be obtained further by submitting Eq. (4) into 1-D Poisson's equation, which gives:

$$BV_{lat} = E_C L_d - \frac{qN_d L_d^2}{2\varepsilon_s}\left[\int_0^{L_d}\left(\int N(x)dx\right)dx - \frac{\eta}{3}\right] \tag{5}$$

Although the Eq. (4)-(5) can be used to depict the influence of arbitrary lateral doping profile on off-state characteristic, only the linear doping profile for the drift region is common and practical in order to obtain the optimized lateral BV. Therefore, in this paper, only the effect of linearly doping profile on the device's off-state characteristic would be discussed thoughtfully, and we will not discuss other cases in detail within the consideration of this paper. It worth to be noted that the Eq. (4)-(5) can also be applied for discrete doped drift region such as Single/Double RESURF cases [4], [15].

III. SURFACE ELECTRIC FIELD

A. SURFACE ELECTRIC FIELD PROFILE

Since the lateral breakdown occurs when the surface electric field peak reaches the critical electric field, the analysis on the surface electric field profile and its sensitivities on structure parameters are essential for the optimization of the device's BV characteristic. For the purpose of achieving a high BV, the lateral power devices are designed that breakdown occurs only when the drift region fully depleted. Therefore, by submitting the actual linear doping profile of the drift region ($N(x) = \varepsilon_s E_C/qt^2 x + N_{d0}$) into Eq. (4), the correspondent surface electric field profile can be given as:

$$E(x) = E_0 - \frac{qN_d}{\varepsilon_s}\left(\frac{kx^2}{2N_d} + \frac{N_{d0}}{N_d}x - \eta\frac{x^2}{2L_d}\right) \tag{6}$$

As Eq. (6) indicates, when $k = k_{ideal}$ and $N_{d0} = 0$, $E(x) = E0$ and a perfectly even surface electric field can be achieved. Yet, as shown in Fig. 4 (a), due to the existence of epitaxial layer doping (N_{d0}), an induced electric field peak at PN junction inevitably appears. The extra charge introduced by N_{d0} curbs the depletion of the drift region, thus reducing the electric field near the NN^+ junction and increase the one at PN junction. Such a surface electric field profile results in a deteriorated lateral BV characteristic. The adjustment of the lateral doping profile is feasible to curb the unfavorable influence of the extra charge. As shown in Fig. 4 (b), by lowing the gradient of lateral doping, the electric field peak at PN junction can be reduced and a new electric field at NN^+ junction may occur making the surface electric field more even.

B. SURFACE ELECTRIC FIELD OPTIMIZATION

To further even the surface electric field and maximize the lateral BV characteristic, the lateral doping profile ought to be optimized in accordance with epitaxial layer impurity and 2-D coupling effect. Since the electric field peak is inevitable, the best scenario is to make the two electric field peaks reach critical electric field simultaneously when lateral breakdown happens, namely:

$$E(0,0) = E(L_d,0) = E_C \tag{7}$$

The correspondent geometric optimization criterion can be given by using Eq. (7) and (6), which yields:

$$N_{d0}/N_d = \eta - 1 \tag{8}$$

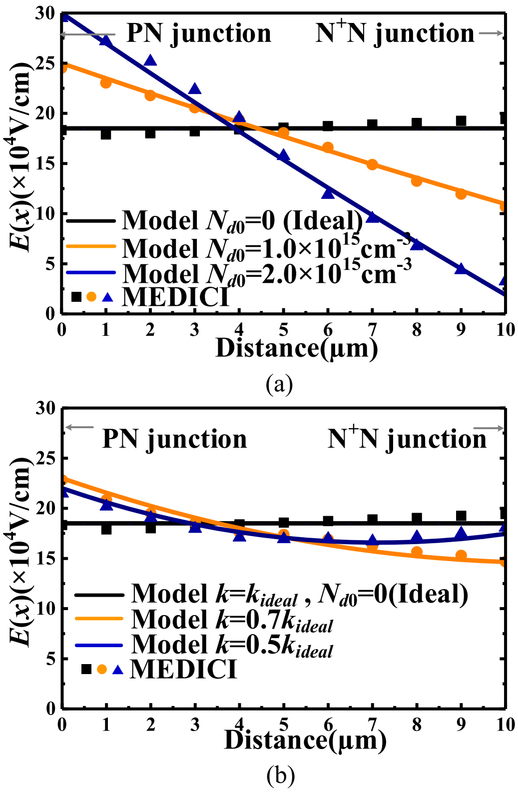

FIGURE 4. Analytical and numerical surface electric field profiles of the drift region for various (a). Epitaxial layer doping concentration (V_{app} = 200V) and (b). Gradient of lateral doping (V_{app} = 200V, $N_{d0} = 1.0 \times 10^{15}\text{cm}^{-3}$) with t_s = 4μm, t_{ox} = 3μm, L_d = 10μm.

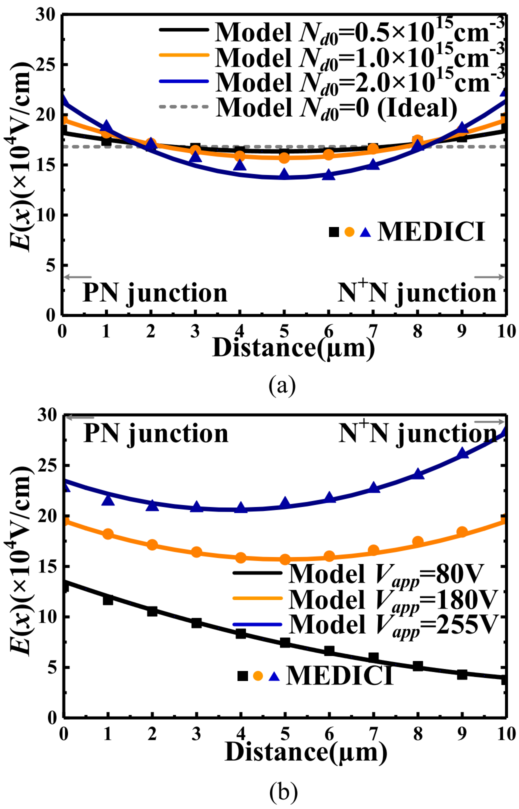

FIGURE 5. Analytical and numerical surface electric field profiles using the optimized gradient of lateral doping for various (a). Epitaxial layer doping concentration (V_{app} = 180V), (b). Applied Voltage ($N_{d0} = 1.0 \times 10^{15}\text{cm}^{-3}$) with t_s = 4μm, t_{ox} = 3μm, L_d = 10μm.

The Eq. (8) indicates that the lateral doping profile is limited by the epitaxial layer impurity and 2-D coupling factor η. For an ideal VLD device ($N_{d0} = 0$), the perfectly even surface electric field achieved when $\eta = 1$. Meanwhile, for a Single-RESURF device, the $N_{d0} = N_d$, thus η ought to equal to 2 so that the symmetric surface electric field along the midline of the drift region can be achieved. Since for the VLD lateral power device, the lateral doping profile is defined by a linear function, the optimized gradient of lateral doping profile can be obtained by submitting $N(x) = kx+N_{d0}$ into Eq. (8), which yields:

$$k_{opt} = \frac{(2-\eta)N_{d0}}{(\eta-1)L_d}, \quad \eta > 1 \tag{9}$$

Fig. 5 intuitively shows the optimized surface electric field profile after using the optimized gradient of lateral doping profile. As shown in Fig. 5 (a) and (b), the results obtained by the proposed model both are found to be sufficiently accurate as compared to simulations. As Eq. (9) indicates that the optimized gradient of drift region doping is a function of drift region length and epitaxial impurity concentration. As shown in Fig. 5 (a), in the case of $\eta > 2$, the optimized k_{opt} is even below zero meaning that the actual doping type ought to be P-type so that the doping concentration at PN junction is higher than that at NN^+ junction. Since the optimized VLD lateral power device has two electric field peaks on the surface, as shown in Fig. 5 (b), the increase of the reverse-applied voltage lifts the peak at the NN+ junction. As mentioned above, it is desirable to make both peaks reach the same height when the lateral breakdown occurs. Nevertheless, as shown in Fig. 4 and 5, the surface electric field profile is a strong function of charge distribution in the drift region. Considering the process tolerance in the fabrication process, in order to increase yields and reduce costs, it is vital to make the device happens vertical breakdown. Especially, in the most desirable case, the lateral and vertical structures reach the breakdown simultaneously. Then the optimized gradient can be further obtained using the expression of vertical voltage ($V_{app} = qN_dt_s/\varepsilon_s(K\eta t_{ox}+\eta t_s-t_s/2)$) and vertical breakdown condition, which yields:

$$k_{opt} = \frac{\varepsilon_s E_C}{qt_sL_d} - \frac{2N_{d0}}{L_d}. \tag{10}$$

IV. BREAKDOWN VOLTAGE

In order to achieve a high BV and maintain a big process tolerance, it is rather essential to optimize the structure parameters of VLT lateral power devices during the design phase. For a lateral power device as shown in Fig. 1(a), breakdown may occur at the surface of the drift region(Point A and B) or Si-SiO_2 interface under the drain region(Point C), its breakdown voltage, therefore, is limited by the lowest among lateral (BV_{lat}) and vertical (BV_{ver}) breakdown voltage, namely:

$$BV = Min[BV_{lat}, BV_{ver}] \tag{11}$$

The vertical breakdown voltage can be easily obtained by using the PN junction breakdown theory, which yields:

$$BV_{ver} = E_C(Kt_{ox} + t_s) - \frac{qN_d t_s^2}{2\varepsilon_s} \tag{12}$$

where $K = \varepsilon_s/\varepsilon_{ox} \sim 3$ is the dielectric constant ratio of silicon and silicon dioxide material, t_s being the epitaxial layer thickness and t_{ox} represents the thickness of the buried oxide layer. Under the premise of full depletion condition, the lateral breakdown voltage of the VLD lateral power devices, on the other hand, can be given by submitting $N(x) = kx + N_{d0}$ into Eq. (5), which yields:

$$\text{PN junction: } BV_{lat}^{FPN} = E_C L_d - \frac{qN_d L_d^2}{2\varepsilon_s}\left(\frac{1}{3} - \frac{\eta}{3} + \frac{2N_{d0}}{3N_d}\right) \tag{13}$$

$$\text{NN}^+ \text{ junction: } BV_{lat}^{FNN} = E_C L_d - \frac{qN_d L_d^2}{2\varepsilon_s}\left(\frac{2\eta}{3} - \frac{2}{3} - \frac{N_{d0}}{3N_d}\right) \tag{14}$$

As discussed in Part III, three possible cases that surface electric field peaks may have: 1). the peak at PN and NN$^+$ junctions have the same height, 2). the peak at PN junction is the highest, and 3). the peak at NN$^+$ junction is the highest. These three cases of surface electric field corresponds to three lateral breakdown cases. As Eq. (13) and (14) indicate, the synchronous breakdown of PN and NN$^+$ junctions occurs when $BV_{lat}^{FPN} = BV_{lat}^{FNN}$. The PN junction breakdown means $BV_{lat}^{FPN} > BV_{lat}^{FNN}$ while NN$^+$ junction breakdown satisfies $BV_{lat}^{FPN} < BV_{lat}^{FNN}$. It is worthy to be noted that, in this paper, the critical electric field (E_C) is determined by $E_C = 3.0\times10^5/[1-0.33log_{10}(N_d/10^{16})]$(V/cm) [4]–[6], [15]. Moreover, although the device's partial depletion breakdown (BV_{lat}^{PPN}) is usually avoided during the design phase for its low breakdown voltage, the proposed method can also be used to depict the electric field profile and BV characteristic. To do so, L_d used in Eq. (4) and (5) ought to be replaced by x_{lat} which is given by $\int E(x)dx = V_{app}$ and $E(x_{lat}) = 0$. As Eq. (13) and (14) indicate, by using the proposed VLD-ECP concept, a simple but accurate analytical expression on the device's breakdown voltage can be obtained easily. As shown in Fig. 6, with the increase of the inherent epitaxial layer impurity, the vertical breakdown is harder to occur. As Eq. (13) indicates, this is because the PN junction breakdown drops as N_d increases making the breakdown tends to occur on the surface rather than on the Si-SiO_2 interface. Since the lateral breakdown is very sensitive to the fabrication-related structure parameters variations, to ensure a good robustness and process tolerance, it is desirable to have the device breakdowns vertically when operates on off-state. Therefore, the designed lateral breakdown voltage ought to be high enough

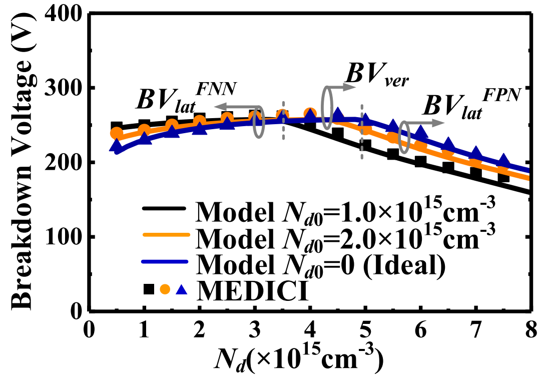

FIGURE 6. **The dependence of breakdown voltage on drift region doping for various Epitaxial layer doping concentration (t_s = 4μm) with t_{ox} = 3μm, L_d = 10μm.**

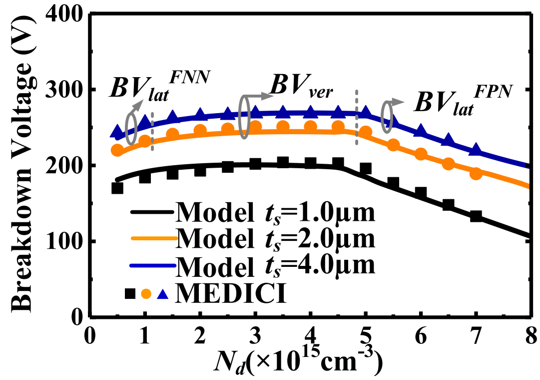

FIGURE 7. **The dependence of breakdown voltage on drift region doping using the optimized gradient of lateral doping for various Epitaxial layer thickness (N_{d0} = 1.0 × 10^{15}cm^{-3}) with t_{ox} = 3μm, L_d = 10μm.**

for a certain set of drift region geometric parameters. Thanks to the simplicity of the proposed methodology, by using the optimized gradient of lateral doping, the maximized lateral breakdown voltage can be obtained easily, which yields:

$$BV_{lat\_MAX} = BV_{lat}^{FPN} = BV_{lat}^{FNN} = E_C L_d - \frac{qN_d L_d^2}{2\varepsilon_s}\left(\frac{\eta}{3} - \frac{1}{3}\right) \tag{15}$$

As shown in Fig. 7, the breakdown of VLT lateral power devices may successively undergo NN$^+$ junction full-depletion, vertical breakdown and PN junction full depletion breakdown with the increase of N_d. However, with the help of the linear doping profile, the high doping concentration near NN$^+$ junction makes it is hard to be depleted. Therefore, the NN$^+$ junction breakdown is very hard to occur allowing a wider range of process tolerance. Apparently, when $N_{d0} = N_d$ and $k = 0$, the Eq. (13) and (14) are degenerate to Single-RESURF case, in which case, the drift region is uniformly doped. While, when $N_{d0} = 0$ and $\eta = 1$, the ideal VLD structure can be achieved. In such a case, the ideal lateral BV characteristic that $BV_{lat}^{FPN} = BV_{lat}^{FNN} = E_C \times L_d$ is therefore obtained.

V. CONCLUSION

In order to elaborate on the physical meaning of the Variation of Lateral Doping (VLD) technique and provide quantitative and qualitative analysis of the VLD lateral power devices at the same time, we proposed a 1-D analytical model for arbitrary lateral doping profile. By using the ECP concept, the inherent 2-D device, which has both 2-D coupling effect and arbitrary lateral doping profile, can be equivalent to a 1-D planar junction with effective concentration profile. Therefore, the 2-D coupling between the RESURF effect and arbitrary doping can be considered simultaneously via the principle of the compensated semiconductor. Moreover, the VLD-ECP concept indicates that the VLD technique obtains the ideal lateral BV characteristic and even surface electric field by realizing a balance between the 2-D coupling effect and drift region doping profile. However, such a perfect balance between 2-D coupling and lateral doping is impossible to be achieved in the real world. Thus, using the proposed VLD-ECP concept and 1-D analytical model, the in-depth discussion on the sensitivity of the surface electric field and breakdown voltage to structure parameters is provided for the first time. Furthermore, we proposed a simple optimization method to compensate the extra charge that introduced by inherent epitaxial layer impurity. So that, the electric field peaks can reach the same height when lateral breakdown occurs. The consistency between the analytical results and the simulations from TCAD tools validates the veracity and effectiveness of the proposed 1-D methodology.

REFERENCES

[1] D. Disney, T. Letavic, T. Trajkovic, T. Terashima, and A. Nakagawa, "High-voltage integrated circuits: History, state of the art, and future prospects," *IEEE Trans. Electron Devices*, vol. 64, no. 3, pp. 659–673, Mar. 2017. doi: 10.1109/TED.2016.2631125.

[2] X. R. Luo *et al.*, "Ultralow ON-resistance high-voltage p-channel LDMOS with an accumulation-effect extended gate," *IEEE Trans. Electron Devices*, vol. 63, no. 6, pp. 2614–2619, Jun. 2016. doi: 10.1109/TED.2016.2555327.

[3] F. Udrea, G. Deboy, and T. Fujihira, "Superjunction power devices, history, development, and future prospects," *IEEE Trans. Electron Devices*, vol. 64, no. 3, pp. 713–727, Mar. 2017. doi: 10.1109/TED.2017.2658344.

[4] Z. Jun *et al.*, "One-dimensional breakdown voltage model of SOI RESURF lateral power device based on lateral linearly graded approximation," *Chin. Phys. B*, vol. 24, no. 2, 2015, Art. no. 028502. doi: 10.1088/1674-1056/24/2/028502.

[5] M. Imam, M. Quddus, J. Adams, and Z. Hossain, "Efficacy of charge sharing in reshaping the surface electric field in high voltage lateral RESURF devices," *IEEE Trans. Electron Devices*, vol. 51, no. 1, pp. 141–148, Jan. 2004. doi: 10.1109/TED.2003.821383.

[6] J. Zhang, Y.-F. Guo, D. Z. Pan, and F.-R. Hu, "A new physical understanding of lateral step doping technique via effective concentration profile concept," *IEEE Trans. Electron Devices*, vol. 66, no. 5, pp. 2353–2358, May 2019. doi: 10.1109/TED.2019.2903346.

[7] Y. Guo, Z. Wang, and G. Sheu, "Variation of lateral thickness techniques in SOI lateral high voltage transistors," in *Proc. Int. Conf. Commun. Circuits Syst.*, Milpitas, CA, USA, 2009, pp. 611–613. doi: 10.1109/ICCCAS.2009.5250456.

[8] I. Cortés, G. Toulon, F. Morancho, E. Hugonnard-Bruyere, B. Villard, and W. J. Toren, "Analysis and optimization of lateral thin-film Silicon-on-insulator (SOI) MOSFET transistors," *Microelectron. Rel.*, vol. 52, no. 3, pp. 503–508, 2012. doi: 10.1016/j.microrel.2011.12.011.

[9] Y. Guo, J. Yao, B. Zhang, H. Lin, and C. Zhang, "Variation of lateral width technique in SoI high-voltage lateral double-diffused metal–oxide–semiconductor transistors using high-k dielectric," *IEEE Electron Device Lett.*, vol. 36, no. 3, pp. 262–264, Mar. 2015. doi: 10.1109/LED.2015.2393913.

[10] A. Ferrara, B. K. Boksteen, R. J. E. Hueting, A. Heringa, J. Schmitz, and P. G. Steeneken, "Ideal RESURF geometries," *IEEE Trans. Electron Devices*, vol. 62, no. 10, pp. 3341–3347, Oct. 2015. doi: 10.1109/TED.2015.2460112.

[11] J. Yao *et al.*, "Analytical model for silicon-on-insulator lateral high-voltage devices using variation of lateral thickness technique," *Jpn. J. Appl. Phys.*, vol. 54, no. 2, 2015, Art. no. 024301. doi: 10.7567/JJAP.54.024301.

[12] B. J. Baliga and S. K. Ghandhi, "Analytical solutions for the breakdown voltage of abrupt cylindrical and spherical junctions," *Solid-State Electron.*, vol. 19, no. 9, pp. 739–744, 1976. doi: 10.1016/0038-1101(76)90152-0.

[13] K. Yang *et al.*, "A novel variation of lateral doping technique in SOI LDMOS with circular layout," *IEEE Trans. Electron Devices*, vol. 65, no. 4, pp. 1447–1452, Apr. 2018. doi: 10.1109/TED.2018.2808193.

[14] Y. Hu *et al.*, "A high-voltage (>600 V) N-island LDMOS with step-doped drift region in partial SOI technology," *IEEE Trans. Electron Devices*, vol. 63, no. 5, pp. 1969–1976, May 2016. doi: 10.1109/TED.2015.2487345.

[15] J. Zhang, Y.-F. Guo, D. Z. Pan, K.-M. Yang, X.-J. Lian, and J.-F. Yao, "Effective doping concentration theory: A new physical insight for the double-RESURF lateral power devices on SOI substrate," *IEEE Trans. Electron Devices*, vol. 65, no. 2, pp. 648–654, Feb. 2018. doi: 10.1109/TED.2017.2786139.